

Spin dynamics of magnetic nanoparticles: Beyond Brown's theory

U. Nowak,^{1,2,*} O. N. Mryasov,¹ R. Wieser,^{1,3} K. Guslienko,^{1,4} and R. W. Chantrell^{1,2}

¹Seagate Research, 1251 Waterfront Place, Pittsburgh, Pennsylvania 15222, USA

²Department of Physics, University of York, York YO10 5DD, United Kingdom

³Institut für Physik, Universität Duisburg-Essen, 47048 Duisburg, Germany

⁴Materials Science Division, Argonne National Laboratory, Argonne, Illinois 60439 USA

(Received 31 August 2005; published 17 November 2005)

An investigation of thermally induced spin dynamics of magnetic nanoparticles is presented. We use an atomistic model for the magnetic interactions within an effective, classical spin Hamiltonian constructed on the basis of first-principles calculations for $L1_0$ FePt. Using Langevin dynamics we investigate how the internal degrees of freedom affect the switching behavior at elevated temperatures. We find significant deviations from a single-spin model, arising from the temperature dependence of the intrinsic properties, from longitudinal magnetization fluctuations, and from both thermal and athermal finite-size effects. These findings underline the importance of atomistic simulations for the understanding of fast magnetization dynamics.

DOI: [10.1103/PhysRevB.72.172410](https://doi.org/10.1103/PhysRevB.72.172410)

PACS number(s): 75.75.+a, 75.10.Hk, 75.20.-g, 75.50.Ss

The fundamental understanding of thermally activated spin dynamics is an important physical problem and a major challenge for a number of magnetic materials and devices. For example, elevated temperatures induced by laser pulses are central to the heat-assisted magnetic recording (HAMR) process,^{1,2} while current induced heating is potentially a problem in magnetic random access memory (MRAM) devices. These technology related phenomena motivate the understanding of pump-probe experiments which are at the forefront of research in magnetodynamics.^{3,4}

The pioneering work of Brown⁵ represents an important basis for the understanding of thermally activated dynamic processes in isolated single-domain particles. The basic idea is that the energy barrier ΔE separating two (meta)stable magnetic states of a nanoparticle can be overcome by thermal activation on a certain time scale which can be calculated within the framework of the stochastic Landau-Lifshitz-Gilbert (LLG) equation. In the limit of low temperatures $k_B T \ll \Delta E$ the escape time τ follows a thermal activation law, $\tau = \tau_0 \exp(\Delta E/k_B T)$, where the prefactor τ_0 as well as the energy barrier ΔE depend on the mechanism of the reversal. As a solvable example, Brown considered an ensemble of isolated magnetic moments with a uniaxial anisotropy in an external magnetic field.⁵ Each single particle of the ensemble is described as one superspin of constant length with uniaxial anisotropy. The superspin is thought to represent the magnetic moment of a whole particle since it was assumed that if the particle is sufficiently small it is always homogeneously magnetized and its microscopic, internal degrees of freedom can be neglected. After the original work of Brown, extensive calculations were performed in order to calculate the energy barrier as well as the prefactor asymptotically for various model systems.⁶⁻¹¹

Experiments on isolated, magnetic particles have confirmed this theoretical approach to thermal activation.¹² However, the use of a single-domain model, especially at high temperatures, has never been rigorously examined. One can identify a number of ways in which the simple single-domain approach cannot represent the effects of the internal

degrees of freedom of a particle. The first of these is the presence of noncoherent reversal modes as they occur, e.g., in elongated nanoparticles.^{10,11,13} Secondly, one must account for the temperature variation of the intrinsic properties. The empirical approach used, for example, by Skomski¹⁴ simply replaces the anisotropy constant and saturation magnetization by temperature-dependent quantities $K(T)$ and $M(T)$. Although this approach is useful, it is not clear *a priori* how well it truly represents the effects of the internal degrees of freedom. For example, for nanomagnetics finite-size effects may profoundly influence the role played by the internal degrees of freedom in magnetization relaxation and other magnetic properties. Finally, as pointed out by Garanin and Chubykalo-Fesenko,¹⁵ the magnetization of the particle is subject to (longitudinal) fluctuations of the magnitude of the magnetization in addition to the transverse fluctuations taken into account by the LLG equation on which ultimately the single-particle model is based. In the following we use an atomistic model which takes explicit account of all these factors. We demonstrate the regime of importance of each of the above manifestations of the internal degrees of freedom and demonstrate the importance of the atomistic approach in the rigorous study of single-particle dynamics.

Although the concepts and models are applicable in general to magnetic nanoparticles, in this work we use as an example FePt, whose temperature dependent dynamics are of special interest because of their potential HAMR applications. We model FePt nanoparticles in the ordered $L1_0$ phase using an effective, classical spin Hamiltonian. This model¹⁶ was constructed on the basis of constrained density functional theory calculations of noncollinear magnetic configurations¹⁷ and site-resolved magnetocrystalline anisotropy.¹⁸ In addition to the commonly considered Heisenberg exchange and single-ion anisotropy, this effective spin Hamiltonian includes coordination-dependent exchange and an effective two-ion anisotropy mediated by the induced magnetic moment of Pt.¹⁶ Both isotropic and anisotropic extra exchange terms are positive and thus stabilize ferromagnetic order along the 001 direction.¹⁹ In order to verify the

form of the Hamiltonian, especially the two-ion anisotropy, equilibrium data for the temperature dependence of the anisotropy constant were compared with experimental data and it has been shown¹⁶ that this model successfully describes the critical temperature and the anomalous temperature dependence of the uniaxial anisotropy energy constant K_1 found experimentally in this ordered alloy.^{20,21}

The model above is used here to investigate the dynamic magnetic properties of FePt nanoparticles. The full Hamiltonian with additional Zeeman energy and dipole-dipole coupling is

$$\begin{aligned} \mathcal{H} = & - \sum_{i < j} (J_{ij} \mathbf{S}_i \cdot \mathbf{S}_j + d_{ij}^{(2)} S_i^z S_j^z) - \sum_i d^{(0)} (S_i^z)^2 \\ & - \sum_{i < j} \frac{\mu_0 \mu^2}{4\pi} \frac{3(\mathbf{S}_i \cdot \mathbf{e}_{ij})(\mathbf{e}_{ij} \cdot \mathbf{S}_j) - \mathbf{S}_i \cdot \mathbf{S}_j}{r_{ij}^3} - \sum_i \mu \mathbf{B} \cdot \mathbf{S}_i, \end{aligned} \quad (1)$$

where the two-ion anisotropy parameters $d_{ij}^{(2)}$ are the dominant contribution to the uniaxial anisotropy energy in relation to the single-ion term $d^{(0)}$. In the classical approximation the spins are three-dimensional unit vectors, μ is the average atomic magnetic moment, the \mathbf{e}_{ij} are unit vectors in the direction connecting lattice sites i and j , and the J_{ij} are effective Fe-Fe exchange integrals. Note, that only the Fe sites are considered as thermal degrees of freedom while the Pt ions are treated effectively in the parameters. The exchange energy, which in our model is not restricted to nearest-neighbor interaction but is taken into account within a distance of up to five atomic unit cells, is calculated via fast Fourier transformation, i.e., it is treated in the same way as the dipolar interaction. We simulate spherical nanoparticles with open boundary conditions and sizes up to $N=1840$ moments, corresponding to diameters up to 4.6 nm. As simulation method we use Langevin dynamics, i.e., simulations of the LLG equation of motion with the dimensionless Gilbert damping parameter $\alpha=1$ (high damping limit) and the gyromagnetic ratio γ . Thermal fluctuations are included as an additional noise term in the internal fields. All algorithms we use are described in detail in Ref. 22.

Our simulations start with all magnetic moments in easy-axis direction. We switch on a magnetic field \mathbf{B} of 2 T antiparallel to the magnetization so that the initial spin state is metastable and the magnetization will reverse after some time. Because of the broad statistical distribution of switching times, averages are taken over 100 simulation runs and the mean switching time τ is comparable to the escape time which follows from analytical considerations.^{11,22,23}

Before presenting results for the switching times itself we analyze the reversal modes of the simulated particles. A good indication of switching by uniform rotation is the time invariance of the length of the magnetization vector. A reversal by other modes like, e.g., thermal nucleation with subsequent domain wall propagation would necessarily lead to a dip of the magnetization during the reversal.²⁴ Therefore, in Fig. 1, time-averaged equilibrium magnetization data are compared with the value of magnetization during switching. Precisely, the latter data represent the absolute value of the magnetiza-

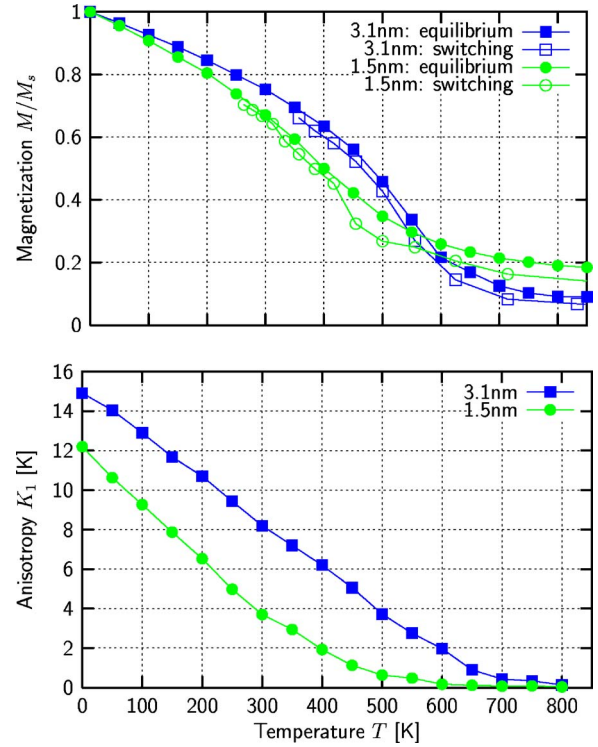


FIG. 1. (Color online) Top: Absolute value of reduced magnetization versus temperature for different particle sizes. Equilibrium values are compared with values during switching. Bottom: Corresponding anisotropy energy constant per spin.

tion of the particle calculated at the switching time, then averaged over 100 switching events. It can be seen that, at least at low temperatures, the value of the magnetization during switching is very close to the equilibrium magnetization curve, indicating coherent reversal. However, at higher temperatures, the dynamic and static magnetization values deviate. It is reasonable to suppose that this occurs because of an increasing importance of longitudinal fluctuations in the hard-axis direction at high temperatures.^{15,25}

It is worth noting that not only does the magnetization show finite-size effects in Fig. 1 but also the anisotropy energy constant $K_1(T)$ calculated as the energy difference between magnetization oriented parallel or perpendicular to the easy axis (see also Ref. 16). One interesting observation here is the size dependence of K_1 even at low temperatures. This nonthermal finite-size effect originates from the exchange-mediated effective two-ion anisotropy which is coordination dependent. The anisotropy energy constant will be the key for the understanding of the dynamic behavior of our system which we will discuss in the following.

Figure 2 shows the temperature dependence of the simulated switching times for particles of different sizes. Also shown for comparison are the analytical asymptotes following the work of Brown,⁵ which in our units are

$$\tau = \frac{1 + \alpha^2}{\alpha \gamma 2d/\mu} \frac{\sqrt{\pi k_B T / Nd}}{(1 - h^2)(1 - h)} \exp \frac{Nd(1 - h)^2}{k_B T}, \quad (2)$$

where $h = \mu B / 2d$ is the reduced magnetic field and d the uniaxial anisotropy parameter. In our model its value follows

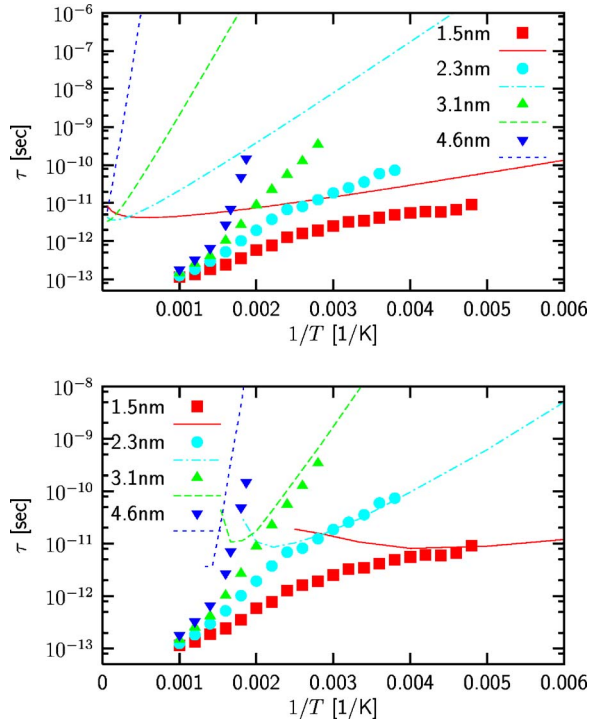


FIG. 2. (Color online) Switching times vs inverse temperature for different particle sizes. Top: Comparison of our numerical data with the escape time following Brown's formula. Bottom: Comparison of the same numerical data with a Brown-type formula where the temperature dependence of $K_1(T)$ and $M(T)$ is taken into account.

from the parameter $d_{ij}^{(2)}$ and $d^{(0)}$ in the Hamiltonian Eq. (1). As we showed before, the reversal mechanism is a uniform rotation and one would expect the Brown asymptote to be an appropriate description for sufficiently low temperatures $k_B T \ll \Delta E$. However, obviously this is not the case even though the above condition is clearly fulfilled (an estimate for the energy barrier yields $\Delta E/k_B \approx Nd/k_B \approx 29\,000$ K for the largest simulated particle).

These deviations are mainly due to the fact that the magnetic nanoparticle itself is a thermodynamic system, with a temperature-dependent magnetization and anisotropy energy. Consequently, the relevant energy barrier is a temperature-dependent free energy barrier $\Delta F(T, B) = \Delta E(T, B) - T\Delta S(T, B)$ with entropy $S(T, B)$. Both magnetization and the anisotropy energy barrier must vanish at the critical temperature, as shown in Fig. 1, leading to $\Delta F(T \rightarrow T_c) \rightarrow 0$. This effect can indeed be found in Fig. 2 also, since data for different sizes converge close to $1/T_c \approx 0.0015$ K.

These thermodynamic effects within the particle itself are not included in Brown's original theory, which leads to the failure shown in Fig. 2. However, as a test of our considerations above we include the thermodynamic behavior of the particle by considering the temperature dependence of the anisotropy energy constant $K_1(T)$ and the magnetization $M(T)$ as calculated in Fig. 1 and putting these simulated equilibrium data into Eq. (2) [$d \rightarrow K_1(T)$, $\mu \rightarrow M(T)$]. With this simple change, the agreement is surprisingly good (Fig. 2, bottom). Note, however, that Brown's asymptote is valid

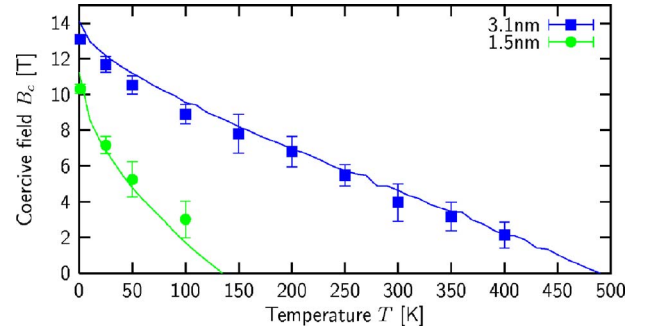


FIG. 3. (Color online) Dynamic coercivity vs temperature for different particle sizes. The solid lines are Eq. (3) where the temperature dependence of $K_1(T)$ and $M(T)$ is taken into account.

only for $k_B T \ll \Delta E(T)$; the apparent deviations at high temperatures are due to a failure of the Brown approximation.

Data for longer time scales and lower temperatures would of course be desirable, but the CPU requirements would be prohibitive. As an alternative, in order to investigate thermal switching for a broader range of temperatures, we calculated the dynamic coercivity. These simulations were performed with a constant field sweeping rate of $dB/dt = 17$ T/ns. The coercive fields were evaluated for different temperatures and averaged over 25 runs. The results are shown in Fig. 3 for different system sizes.

For finite temperatures the coercive field is drastically reduced, approaching zero for temperatures far below the Curie temperature. In order to establish once again the importance of the thermodynamic behavior of the particle quantitatively, we compare our data with a simple formula which can be deduced from Eq. (2), simplifying the prefactor to a constant τ_0 and solving the equation for the coercive field depending on time scale and temperature,

$$B_c(\tau, T) = \frac{2K_1(T)}{M(T)} \left(1 - \sqrt{\frac{k_B T}{NK_1(T)} \ln(\tau/\tau_0)} \right). \quad (3)$$

Once again, the agreement is rather good, considering the simplifications in Eq. (3).

In summary, we have used an effective spin model to study relaxation processes in an isolated nanoparticle, explicitly including the internal degrees of freedom. The model has been used to investigate the limits of the single-spin relaxation theory of Brown.⁵ We have shown that the time scales for thermally activated switching deviate strongly from the asymptotes as calculated within the framework of Brown's theory. As we showed, these deviations result from the particles internal degrees of freedom. Especially at the Curie temperature the energy barriers must vanish. Taking this into account we show that the switching behavior can be understood in terms of simple thermal activation laws but with the equilibrium temperature dependence of the magnetic anisotropy energy constant and the magnetization. This finding suggests that there is a strong justification for the use of empirical approaches such as those of Skomski¹⁴ even, perhaps surprisingly, in the case of high frequencies and high temperatures where the disorder is large. However, the use of empirical approaches must be tempered by our finding of a

significant finite-size effect, specifically the effect of finite size on $K(T)$ for layered ferromagnets of the $L1_0$ type. This dramatic effect is a direct consequence of the reduction in coordination number on the (Pt mediated) two-ion anisotropy constant, and must be considered an important consideration in the behavior of FePt nanoparticles, especially in terms of the determination of their thermal stability.

We should note that Brown's theory should still be applicable for sufficiently low temperatures. However, in a temperature range between room temperature and T_c , realistic switching times may deviate by many orders of magnitude. This striking feature underlines the relevance of our findings for the estimate of the superparamagnetic limit as well as for HAMR applications. Finally our calculations show the effects of longitudinal fluctuations of the magnetization at high temperatures. These are evident in the difference in static and dynamic magnetization as demonstrated in Fig. 1. The difference is pronounced for nanoparticles of 1.5 nm diameter. We would expect that the longitudinal fluctuations would affect the energy barrier and hence the relaxation time. How-

ever, these differences would be apparent at very small values of KV/kT , where the Brown expression is invalid. In order to quantify this effect, one would need comparison with some asymptote valid in the limit of low energy barriers, and also many numerical calculations, in order to achieve statistical accuracy, and this is beyond the scope of the current work. Nevertheless, our findings underline the validity and the importance of atomistic simulations for the understanding of thermally activated spin dynamics, in particular the role of longitudinal magnetization fluctuation close to the Curie temperature.

We are grateful to O. Chubykalo-Fesenko for fruitful discussions. Work at Seagate Research was supported by the INSIC HAMR ATP Program, the U. S. Department of Commerce, NIST, ATP Cooperation Agreement, No. 70NANB1H3056, at ANL by US DOE BES Grant No. W-31-109-ENG-38, and at Duisburg by the Deutsche Forschungsgemeinschaft (SFB 491).

*Electronic address: un500@york.ac.uk

¹S. Cumpson, P. Hidding, and R. Coehoorn, IEEE Trans. Magn. **36**, 2271 (2000).

²A. Lyberatos and K. Y. Guslienko, J. Appl. Phys. **94**, 1119 (2003).

³E. Beaurepaire, J.-C. Merle, A. Daunois, and J. Y. Bigot, Phys. Rev. Lett. **76**, 4250 (1996).

⁴J. Hohlfeld, E. Matthias, R. Knorren, and K. H. Bennemann, Phys. Rev. Lett. **78**, 4861 (1997).

⁵W. F. Brown, Phys. Rev. **130**, 1677 (1963).

⁶A. Aharoni, Phys. Rev. **177**, 793 (1969).

⁷W. T. Coffey, D. S. F. Crothers, J. L. Dormann, L. J. Geoghegan, and E. C. Kennedy, Phys. Rev. B **58**, 3249 (1998).

⁸J. L. García-Palacios and P. Svedlindh, Phys. Rev. Lett. **85**, 3724 (2000).

⁹R. W. Chantrell, N. Walmsley, J. Gore, and M. Maylin, Phys. Rev. B **63**, 024410 (2000).

¹⁰H. B. Braun, Phys. Rev. Lett. **71**, 3557 (1993).

¹¹D. Hinzke and U. Nowak, Phys. Rev. B **61**, 6734 (2000).

¹²W. Wernsdorfer, E. B. Orozco, K. Hasselbach, A. Benoit, B. Barbara, N. Demoncey, A. Loiseau, H. Pascard, and D. Mailly, Phys. Rev. Lett. **78**, 1791 (1997).

¹³M. Bode, O. Pietzsch, A. Kubetzka, and R. Wiesendanger, Phys. Rev. Lett. **92**, 067201 (2004).

¹⁴R. Skomski, J. Phys.: Condens. Matter **15**, R841 (2003).

¹⁵D. A. Garanin and O. Chubykalo-Fesenko, Phys. Rev. B **70**, 212409 (2005).

¹⁶O. N. Mryasov, U. Nowak, K. Guslienko, and R. W. Chantrell, Europhys. Lett. **69**, 805 (2005).

¹⁷O. N. Mryasov, V. A. Gubanov, and A. I. Liechtenstein, Phys. Rev. B **45**, 12330 (1992).

¹⁸A. B. Shick *et al.*, Phys. Rev. B **67**, 172407 (2003).

¹⁹O. N. Mryasov, J. Magn. Magn. Mater. **272–276**, 800 (2004).

²⁰S. Okamoto, N. Kikuchi, O. Kitakami, T. Miyazaki, Y. Shimada, and K. Fukamichi, Phys. Rev. B **66**, 024413 (2002).

²¹J.-U. Thiele, K. R. Coffey, M. F. Toney, J. A. Hedstrom, and A. J. Kellock, J. Appl. Phys. **91**, 6595 (2002).

²²U. Nowak, in *Annual Reviews of Computational Physics IX*, edited by D. Stauffer (World Scientific, Singapore, 2001), p. 105.

²³U. Nowak, R. W. Chantrell, and E. C. Kennedy, Phys. Rev. Lett. **84**, 163 (2000).

²⁴D. Hinzke and U. Nowak, Phys. Rev. B **58**, 265 (1998).

²⁵N. Kazantseva, R. Wieser, and U. Nowak, Phys. Rev. Lett. **94**, 037206 (2005).